**Table II.** Structural and Magnetic Parameters for $[CrCl_3]^-$ Chain Compounds

| compd | M–M (intrachain), Å | M–B–M, deg | M–M′ (interchain), Å | Θ, K | $J/k$, K | $T_N$, K | $g$ | $\|J'\|/\|J\|$ | ref |
|---|---|---|---|---|---|---|---|---|---|
| $CsCrCl_3$ | 3.112 | 76.20 | 7.256 | | −24.0 | 16 | | $3 \times 10^{-3}$ | 12 |
| | | | | | −38.2 | | 1.98 | | 20 |
| | | | | | −26.5 | | 1.98 | | 21 |
| $[(CH_3)_4N]CrCl_3$ | 3.256 | 79.00 | 9.129 | −158 | −15.2 | 7 | | $10^{-3}$ | 5 |
| $[(CH_3)_4N]CrBr_3$ | 3.40 | | 9.40 | −124 | −13.1 | | | | this work |

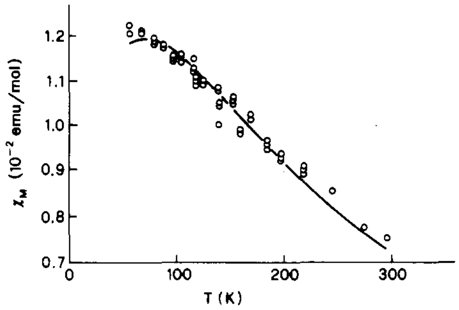

**Figure 2.** Molar magnetic susceptibility $\chi_M$ vs. temperature in the range 50 K to room temperature. The solid line is a fit of the data to the Smith and Friedberg equation.

complexes.[5,12–15] This behavior can be explained by assuming a direct overlap of the $t_{2g}$ orbitals between the nearest-neighbor chromium(II) ions. The antiferromagnetic exchange can arise not only by direct overlap of the $t_{2g}$ orbitals but also by a superexchange mechanism via $e_g$–s–$e_g$ interactions. Ferromagnetic superexchange interactions involving the Br 4p orbitals are also present.[16] The fact that the overall interaction is antiferromagnetic indicates that the exchange is mainly due to the first two contributions. In addition, if we compare the $J$ values, found in $CsCrCl_3$[12] and $[(CH_3)_4N]CrCl_3$[5] (compounds where the *intra*chain Cr–Cr distance increases from 3.11 to 3.26 Å) (see Table II), with that found in our compound (*intra*chain Cr–Cr distance 3.40 Å), we observe a decrease of the antiferromagnetic interactions, due to the decrease of the $t_{2g}$–$t_{2g}$ direct overlap. On the other hand, the ferromagnetic superexchange contribution should become more important because there is an increase of chromium–halogen covalency, in going from the chloride to the bromide derivative.

Below 40 K, the magnetic susceptibility deviates considerably from that expected for an antiferromagnetic chain, and it increases steadily in value up to the lowest temperature accessible to us, i.e. 1.8 K. Magnetization measurements, at the same temperature, made in fields up to 7 T (see Figure 3) show a downward curvature at higher fields, but no saturation was reached. Similar behavior has been observed in other sensitive linear-chain compounds, and the suggestion has been made that it arises from magnetic impurities.[17] In the present case, one possible source of these impurities may be a very small fraction of ferromagnetic $CrBr_3$ ($T_c$ = 36 K),[18] but this possibility can be ruled out because no saturation was observed. The other possibility is the presence of paramagnetic impurities (estimated to be on the order of 3%).[19]

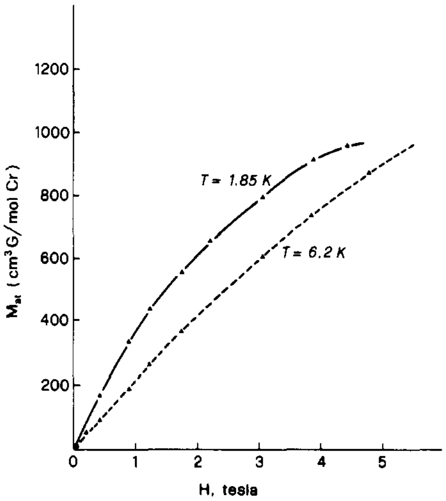

**Figure 3.** Magnetization vs. external magnetic field of $[(CH_3)_4N]CrBr_3$ at 1.8 K (–Δ–Δ) and 6.2 K (- - -Δ- - -Δ).

The three-dimensional magnetic ordering temperature, $T_N$, has not been detected, possibly due to the masking effect of the impurities. The temperature $T_N$, if present, is expected to lie below 7 K, the observed value for $[(CH_3)_4N]CrCl_3$,[5] and this is because of the presence of a longer *inter*chain distance.

**Acknowledgment.** We wish to thank P. Filaci for technical assistance and M. Viola for drawings.

**Registry No.** $[(CH_3)_4N]CrBr_3$, 29794-92-1; Cr, 7440-47-3; HBr, 10035-10-6.

---

(12) Day, P.; Gregson, A. K.; Leech, D. H.; Hutching, M. T.; Rainford, B. D. *J. Magn. Magn. Mater.* **1979**, *14*, 166.
(13) McPherson, G. L.; Kistenmacher, J. J.; Floker, J. B.; Stucky, G. D. *J. Chem. Phys.* **1972**, *57*, 3771.
(14) Crama, W. J.; Baker, M.; Maaskant, W. J. A.; Veschoor, C. G. *Acta Crystallogr., Sect. B: Struct. Crystallogr. Cryst. Chem.* **1979**, *B35*, 1875.
(15) Crama, W. J.; Maaskant, W. J. A.; Veschoor, C. G. *Acta Crystallogr., Sect. B: Struct. Crystallogr. Cryst. Chem.* **1978**, *B34*, 1973.
(16) Goodenough, J. B. "Magnetism and Chemical Bond"; Interscience: New York, 1963.
(17) Niel, M.; Cros, C.; Chaminade, J. P.; Pouchard, M. *J. Solid State Chem.* **1977**, *20*, 1.
(18) Dillon, J. F., Jr. *J Phys. Soc. Jpn.* **1966**, *19*, 1662.
(19) The percent impurities was estimated by assuming that the magnetic susceptibility in the temperature range 1.8–5 K was completely due to paramagnetic Cr(II) ion impurities.
(20) Larkworthy, L. F.; Trigg, J. K.; Yavari, A. *J. Chem. Soc., Dalton Trans.* **1975**, 1879.
(21) Leech, D. H.; Machin, D. J. *J. Chem. Soc., Dalton Trans.* **1975**, 1609.

---

Contribution from the Chemistry Department,
University of Wisconsin—Madison, Madison, Wisconsin 53706

## Direct Observation of the Boron–Boron Coupling and High-Resolution Proton and Boron Spectra of Diborane

Thomas C. Farrar* and Gregory R. Quinting

*Received August 14, 1984*

Proton and boron-11 spectra of diborane have been previously reported,[1–4] but by today's standards, the resolution was limited. Useful experimental evidence was, however, obtained for the direct $^{11}B$–$^{10}B$ spin coupling constant.[1,2,4] Reasonably accurate estimates of the coupling constants not directly observable were obtained by fitting observed and computer-calculated $^1H$ and $^{11}B$ spectra.[1,2] The quality of these estimates was limited because of the dispersion and resolution of early spectrometers. The direct $^{11}B$–$^{11}B$ coupling

---

(1) Farrar, T. C. *Ann. N.Y. Acad. Sci.* **1966**, *137*, 323.
(2) Farrar, T. C.; Johannesen, R. B.; Coyle, T. D. *J. Chem. Phys.* **1968**, *49*, 281–285.
(3) Gaines, D. F.; Schaeffer, R.; Tebbe, F. *J. Phys. Chem.* **1963**, *67*, 1937–1938.
(4) Odom, J. D.; Ellis, P. D.; Lowman, D. W.; Gross, M. H. *Inorg. Chem.* **1973**, *12*, 95–97.
(5) Shapiro, I.; Weiss, H. G.; Schmich, M.; Skolnik, S.; Smith, G. *J. Am. Chem. Soc.* **1952**, *74*, 901–905.

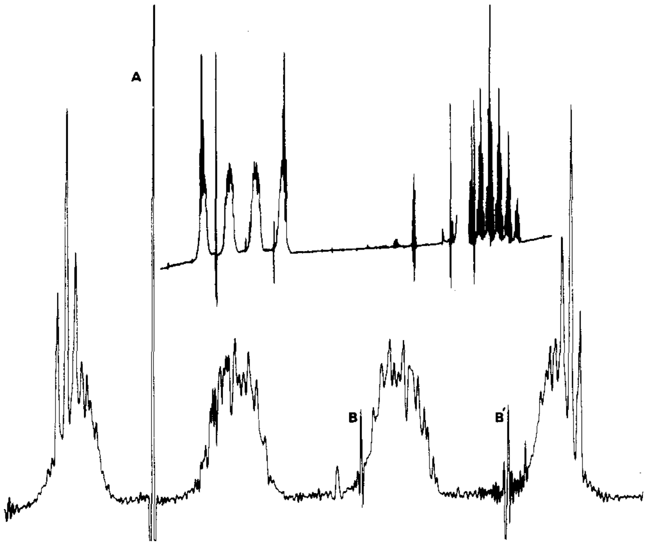

**Figure 1.** 270.13-MHz proton spectrum of $^{11}B_2H_6$ (terminal portion, 600-Hz plot, resolution enhanced): A, ethane impurity peak; B and B', folded-in residual solvent peaks. Inset: Full spectrum showing bridge region.

constant, which is of special interest, could not be observed directly but was indirectly deduced from the calculated spectra. In this paper we report the direct measurement of the $^{11}B$–$^{10}B$ coupling constant in diborane from a completely proton-decoupled $^{10}B$ spectrum. Direct measurements of the bridge proton–boron ($J(BH_b)$) and bridge proton–terminal proton ($J(H_bH_t)$) coupling constants were also obtained. The other coupling constants were obtained by fitting calculated spectra to experimental, resolution-enhanced proton and boron spectra.

## Experimental Section

$^{11}B$-enriched diborane (97%) was prepared by $LiAlH_4$ reduction of $^{11}BF_3$·THF in diglyme.[4] $LiAlH_4$, obtained from Alfa Products Inc., was purified by recrystallization from ethyl ether. $^{11}BF_3$·$(CH_3)_2O$, 97% $^{11}B$-enriched, purchased from Eagle-Picher Inc., was treated with excess tetrahydrofuran, THF, to produce the $^{11}BF_3$·THF complex, which was subsequently purified by vacuum distillation. In the $LiAlH_4$ reduction of the $^{11}BF_3$·THF to yield diborane, the higher boiling THF byproduct was easily separated from the product by high-vacuum fractional condensation.[6]

Approximately 0.2 mmol of purified diborane was condensed into a medium-wall 5-mm NMR tube along with 0.9 mL of degassed $Me_4Si$-$d_{12}$ to obtain a solution concentration of 0.2 M. A second sample was prepared with toluene-$d_8$ as the solvent; each was flame sealed under vacuum. Normal diborane, obtained from laboratory stock, was purified and prepared similarly.

Proton and $^{11}B$ NMR spectra were obtained on an IBM WP-270SY specrometer operating at 270.13 and 86.67 MHz, respectively. Coupled proton spectra were obtained at both 0 and 30 °C. All proton spectra were recorded at 30 °C. Probe temperature regulation was maintained by using manufacturer supplied equipment. A JEOL FX-200 spectrometer was used to acquire the proton-decoupled $^{10}B$ spectra at 21.40 MHz.

For the proton and boron-11 spectra, line-narrowing Gaussian multiplication was applied to the time domain data before Fourier transformation. A positive exponential in combination with trapezoidal weighting was used for resolution enhancement of the boron-10 spectra.

## Results and Discussion

Figure 1 shows the terminal portion of the fully coupled, resolution-enhanced proton spectrum of boron-11-enriched diborane. Figure 2 shows the resolution-enhanced fully coupled boron-11 spectrum. Both spectra were recorded at 30 °C. In a fully coupled proton spectrum taken at 0 °C, the line widths were unchanged from the spectrum taken at 30 °C. Since the proton and boron-11 relaxation times (and line widths) are almost constant in the temperature range −20 to +30 °C, it is clear that the relaxation is due to approximately equal contributions of the dipole–dipole and spin rotation mechanisms. Since the two mechanisms have opposite temperature dependences, the total relaxation time, and hence the line widths, remain almost constant between −20 and +30 °C.

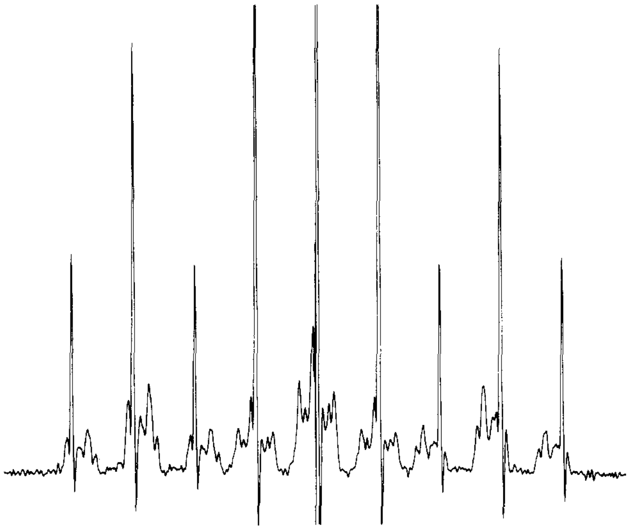

**Figure 2.** 86.7-MHz boron-11 spectrum of $^{11}B_2H_6$ (800-Hz plot, resolution enhanced).

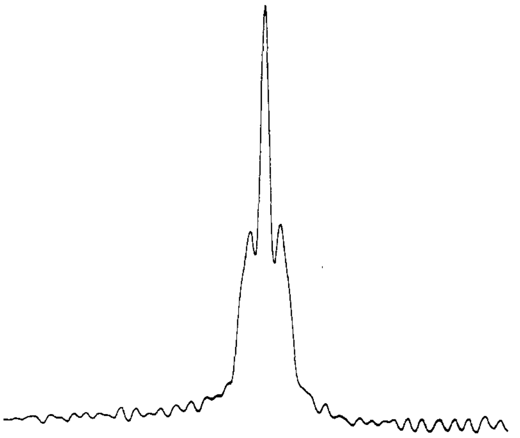

**Figure 3.** 21.40-MHz boron-10 spectrum of $B_2H_6$ (proton decoupled, 62.5-Hz plot, resolution enhanced).

The effects of spin rotation relaxation are very pronounced in the gas-phase proton NMR spectrum of diborane. In this case the proton relaxation time, $T_1$, is less than 1 ms for a sample pressure of 100 torr. The bridge and terminal protons still appear, but as separate, broad spectral peaks; no fine structure is visible because the relaxation time is short.

Proton spectra of $^{11}B$-enriched diborane in toluene-$d_8$ showed considerably larger line widths than in $Me_4Si$-$d_1{}^2$. Since toluene is significantly more viscous than $Me_4Si$, the solute correlation times are much longer. Consequently, the proton spin lattice relaxation time is relatively short. This gives rise to broader lines in toluene solution.

The completely proton-decoupled $^{10}B$ spectrum is shown in Figure 3. The apparent triplet is actually a superposition of a singlet and a quartet. Of an isotopically normal diborane sample 80% is $^{11}B$ and 20% $^{10}B$. Hence, 64% of the diborane molecules are doubly labeled $^{11}B$, 32% are $^{10}B$–$^{11}B$, and 4% are doubly labeled $^{10}B$. In the proton-decoupled $^{10}B$ spectrum, the 1:1:1:1 quartet is due to coupling to the spin $^3/_2$ $^{11}B$ in the $^{10}B$–$^{11}B$ molecules. Under complete proton-decoupling conditions, both boron-10 nuclei are equivalent; therefore, no coupling between $^{10}B$ and $^{10}B$ is observed, giving rise to the singlet part of the spectrum. A simple analysis of this observed $^{10}B$ spectrum gives the $^{10}B$–$^{11}B$ coupling constant: $J(^{10}B$–$^{11}B) = 1.3$ Hz. Consequently, the $^{11}B$–$^{11}B$ coupling constant, $J(^{11}B$–$^{11}B)$, is 3.8 ± 0.2 Hz. This value was used in the final, calculated spectra.

---

(6) The diborane yield was 3.45 mmol (approximately 50%).

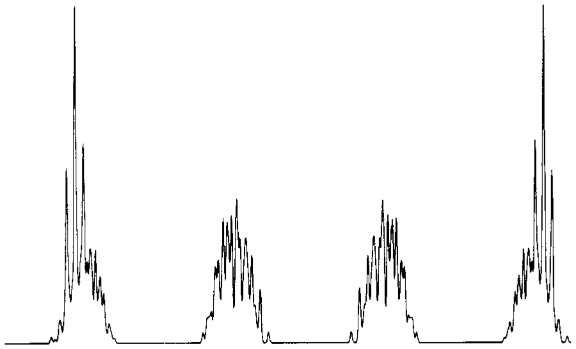

**Figure 4.** Calculated 270.13-MHz proton spectrum of $^{11}B_2H_6$. (See Table I for parameters.)

**Table I.** Optimum *J* Coupling Values (Hz) for Calculated $B_2H_6$ $^1H$ and $^{11}B$ Spectra

| | | | |
|---|---|---|---|
| $J(^{11}B-^{11}B)$ | $\pm 3.8 \pm 0.5^{*a,b}$ | $\lvert J(H_b-H_t)\rvert$ | $7.45 \pm 0.5^{*a,c}$ |
| $\lvert J(^{11}B-H_b)\rvert$ | $46.3 \pm 0.5^{*a}$ | $J(H_t-H_t)$(cis or trans) | $\pm 14.8 \pm 1.0^d$ |
| $J(^{11}B-H_t)$ | $+133.5 \pm 1.0$ | $J(H_t-H_t)$(trans or cis) | $\pm 4.5 \pm 1.0^d$ |
| $J'(^{11}B-H_t)$ | $+4.0 \pm 1.0$ | $\lvert J(H_t-H_t)(gem)\rvert$ | $4.5 \pm 1.0$ |

[a] Key: $H_t$, terminal proton; $H_b$, bridge proton; *, directly measured. [b] The sign of *J*(B–B) can be either negative or positive; it has the same sign as *J*(H–H)(cis and trans). [c] Reversing the sign of $J(H_b-H_t)$ has no effect on the calculated spectrum. [d] Same comment as footnote *b*.

## Calculated Spectra

SPINNAKER (spin polarization intensities of numerous Nuclei analyzed by key eigenvector rotations), a modified version of the UEANMRII NMR simulation program,[7-9] was used to calculate the $^{11}B$ and $^1H$ spectra. SPINNAKER is capable of calculating spectra for systems containing nuclei with spins greater than $^1/_2$ and makes use of symmetry. The present version can accommodate up to seven spins of any spin quantum number or up to seven groups of equivalent spin $^1/_2$ nuclei (e.g., a $CH_3$ group is treated as a single group spin with a group spin quantum number of $^3/_2$). All the calculations here were done with an IBM S-9000 computer. Source programs are available on request.

Most often, iterative calculations are used to achieve an optimum fit between computed and experimental spectra. An iterative procedure was not possible in the case of diborane, however, because its proton and boron spectra consist of several thousand transitions, all of which were not resolved. Several trial sets of coupling constants were used in the computations until an optimum fit to the experimental spectrum was achieved. Only those coupling constants for which a direct measuement was not possible were varied. The directly observed parameters were $J(H_bH_t) = 7.45$ Hz, $J(B-B) = 3.8$ Hz, $J(BH_b) = 46.3$ Hz, and $|J(BH_t) + J'(BH_t)| = 137.5$ Hz. Unless $J(^{11}B-^{11}B) > 0$, no combination of the other coupling constants produced a calculated proton spectrum that came even close to matching the observed spectrum. Furthermore, if the value of *J*(B–B) was changed by more than ±0.5 Hz from its directly measured value of 3.8 Hz, no reasonable fit could be obtained.

The closet fit of calculated to experimental proton and boron-11 spectra was obtained with the $J(H_t-H_t)$(cis and trans) and *J*(B–B) having the same relative signs. In particular, the fine structure near the three main middle peaks in the calculated $^{11}B$ spectrum clearly fits the experimental spectrum best when the relative signs of the three couplings were identical. *J*(H–H)(geminal) had the greatest influence on these same features, yet it had no effect on other parts of the calculated $^{11}B$ spectrum.

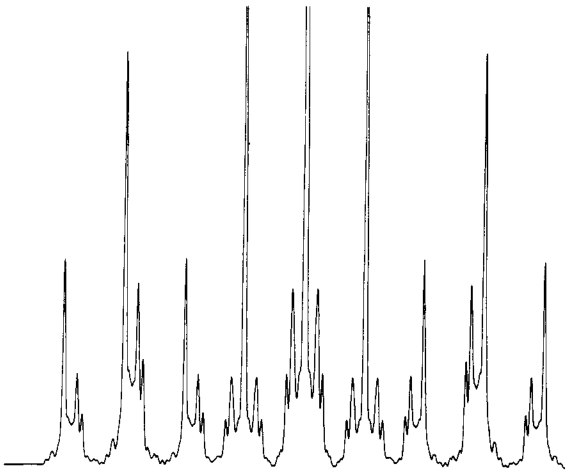

**Figure 5.** Calculated 86.7-MHz boron-11 spectrum of $^{11}B_2H_6$. (See Table I for parameters).

Figures 4 and 5 show the calculated fully coupled $^{11}B$ and $^1H$ spectra that gave the closet fit to the experimental spectra. Minor discrepancies remain that are due to error in the three, less critical cis, trans, and geminal proton–proton couplings. Table I summarizes the chemical shift and coupling parameters that correspond to the best fit, calculated spectra.

The experimental and calculated results reported here agree well with some of those reported earlier.[1,2] The present results are not, however, in such good agreement with those reported in ref 4. Odom and co-workers[4] obtain an *upper limit* of the $^{11}B-^{11}B$ spin coupling constant of 1.1 ± 0.2 Hz, on the basis of a series of elegant multiple-resonance experiments. We can only speculate on the difference between our values and theirs. In our view, the most plausible explanation is the greatly improved sensitivity, resolution, and dispersion of modern high-field FT NMR instruments compared to those used by Odom over 12 years ago (in 1972).

## Conclusions

Because of its small size and simplicity, diborane is an attractive model compound for a variety of theoretical studies, including calculations of the proton and boron-11 chemical shifts and coupling constants. The present studies provide clear experimental results that unequivocally demonstrate that for diborane *J*(B–B) > 0. The results presented here provide reasonably precise values for most of the NMR parameters and can be used as experimental bench marks for future theoretical work.

**Acknowledgment.** We thank Prof. Donald F. Gaines and Darrell E. Coons for helpful discussions throughout this work and for providing the isotopically normal diborane sample. We thank Geoffrey S. Sobering and Emil Y. Sidky for their work on the SPINNAKER program. This work was supported by National Science Foundation Grant CHE-8306696.

**Registry No.** $B_2H_6$, 19287-45-7; $^{10}B$, 14798-12-0.

---

(7) Castellano, S.; Bothner-By, A. A. *J. Chem. Phys.* **1964**, *41*, 3863–3869.

(8) Johannesen, R. B.; Ferretti, J. A.; Harris, R. K. *J. Magn. Reson.* **1970**, *3*, 84–94.

(9) Harris, R. K.; Woodman, C. M. *Mol. Phys.* **1966**, *10*, 437–449.

---

Contribution from the Department of Chemistry,
Howard University, Washington, D.C. 20059

## Kinetic and Equilibrium Study of the Monomer–Dimer Reaction of [Tetrakis(*p*-(trimethylammonio)phenyl)porphinato]silver(III) in Aqueous Medium

M. Krishnamurthy* and John R. Sutter*

*Received September 5, 1984*

The aggregation of porphyrins and porphyrin-like molecules has been the subject of several recent reports.[1-4] Not only do

---

(1) H. Scheer and J. J. Katz in "Porphyrins and Metalloporphyrins", K. M. Smith, Ed., Elsevier, New York, 1975, p 494.